Soil Dynamics and Earthquake Engineering 122 (2019) 274–289

Contents lists available at ScienceDirect

Soil Dynamics and Earthquake Engineering

journal homepage: www.elsevier.com/locate/soildyn

Cyclic behavior and liquefaction resistance of silty sands with presence of initial static shear stress

Xiao Wei[a,b], Jun Yang[a,*]

[a] Department of Civil Engineering, The University of Hong Kong, Hong Kong, China
[b] Key Laboratory of Soft Soil Engineering, Zhejiang University, Hangzhou, China

ARTICLE INFO

Keywords:
Critical state theory
Cyclic loading
Initial shear stress
Liquefaction
Silty sands

ABSTRACT

The liquefaction resistance of silty sands and the potential effect of initial static shear stress are major concerns in seismic design of dams and embankments. This paper presents a systematic experimental study on non-plastic silty sands to address these concerns. It is shown that the concept of threshold α (α_{th}) proposed by Yang and Sze (2011) to characterize the impact of α (representing the initial static shear stress level) on cyclic resistance (*CRR*) of clean sands is applicable to silty sands as well. When $\alpha < \alpha_{th}$, *CRR* increases with increasing α, otherwise it decreases with increasing α. The threshold α is affected by the initial packing density, the initial effective confining pressure and the fines content. An improved state dependency of the threshold α, which is regardless of fines content, is proposed in the framework of critical state soil mechanics by using the state parameter (ψ). An analysis platform, known as *CRR*-ψ platform and developed based on clean sand data, is shown to have the capability of characterizing the state dependence of *CRR* for sands with varying fines contents. This platform in conjunction with the unified α_{th}-ψ correlation provides a unified and consistent framework for understanding the complicated effects of initial static shear stress on soil liquefaction and for quantifying such effects for engineering practice.

1. Introduction

Soil liquefaction has become an important subject area and been investigated for decades since the Niigata earthquake of 1964. Extensive investigations have been conducted based on reconstituted specimens subjected to two-way symmetrical cyclic shear stress (Fig. 1(a)), and revealed that a number of factors (e.g. packing density, effective overburden pressure, loading history, soil fabric, *etc*.) can affect the cyclic behavior and liquefaction resistance of sands. The symmetric cyclic loading condition mainly represents the free-field level ground during an earthquake [2,3]; however, it is not applicable to major geotechnical applications involving dams and embankments [1,4–6] or buildings and heavy structures [7,8], in which initial static shear stress (τ_s) plays an important role in liquefaction analysis. To replicate such loading conditions with the presence of τ_s in triaxial tests, a specimen needs to be consolidated anisotropically to yield an initial static shear stress on the maximum shear stress plane [5,9–12] and loaded by applying asymmetrical stress cycles as a result of superimposition of the initial static shear stress and the uniform shear stress cycles (Fig. 1(b) and (c)). The level of initial static shear stress is usually represented by a normalized parameter α, defined as the ratio between the initial static shear stress and the effective overburden pressure.

Earlier studies on the effect of initial static shear stress showed that the effects of initial static shear stress can be either beneficial (e.g. [9]) or detrimental (e.g. [7]). Seed and Harder [13] and Harder and Boulanger [6] compiled literature data and suggested that the effect of α is positive for dense sand with a relative density of 55–70%, and negative for loose sand with a relative density of around 35%, giving the medium dense sand (45–50%) in between. This proposal is limited to an effective overburden pressure less than 300 kPa and α values less than 0.3. Due to the poor convergence and consistency in the database and analysis, the National Center for Earthquake Engineering Research (NCEER) did not recommend any proposal to be used by non-specialists or in routine engineering practice, but suggested the need for continued research on this issue [14].

* Corresponding author.
E-mail address: junyang@hku.hk (J. Yang).

https://doi.org/10.1016/j.soildyn.2018.11.029
Received 15 January 2018; Received in revised form 20 September 2018; Accepted 29 November 2018
Available online 21 December 2018

Nomenclature

CSL	Critical state line
CRR	Cyclic resistance ratio
CSR	Cyclic stress ratio
DA	Double amplitude
e (e_c)	Void ratio (after consolidation)
e_Γ	Intercept of critical state line in the e-$(p'/P_a)^{0.6}$ plane
FC	Fines content
FC_{th}	Threshold fines content
K_α	Correction factor for initial static shear stress
N_l	Number of cycles to liquefaction/failure
p'	Mean effective stress
P_a	Reference pressure equaling to atmospheric pressure
q_{cyc}	Amplitude of deviatoric stress cycles
q_s	Initial static deviatoric stress
TS	Toyoura sand
TSS10, TSS20	Toyoura sand mixed with crushed silica silt at FC = 10% and 20%
α	Initial static shear stress ratio
α_{th}	Threshold α
Δu	Excess pore water pressure
ε_a	Axial strain
λ_c	Gradient of critical state line in the e-$(p'/P_a)^{0.6}$ plane
σ'_{1c}, σ'_{3c}	Axial and lateral effective stress after consolidation
σ'_{nc}	Normal effective stress on the 45° plane after consolidation
ψ	State parameter

Although some researchers found that the effects of α on the cyclic resistance of sands can be affected by the packing density (e.g. [8,15,16]) and the effective overburden pressure (e.g. [5,17,18]), there was not a unified method for characterizing these effects until that Yang and Sze [1] conducted a comprehensive testing program to investigate the uncertainties about the effects of initial static shear stress. A concept, referred to as threshold α (α_{th}), was proposed by Yang and Sze [1], below which the cyclic resistance increases with increasing α, whereas beyond which the cyclic resistance decreases with further increase of α. An important feature of α_{th} is that it decreases with decreasing packing density and with increasing initial effective confining pressure. Such feature can be characterized by the state parameter (ψ) [19] thus leading to a linear relationship that α_{th} decreases with increasing initial state parameter of sand specimens. In addition, Yang and Sze [20]

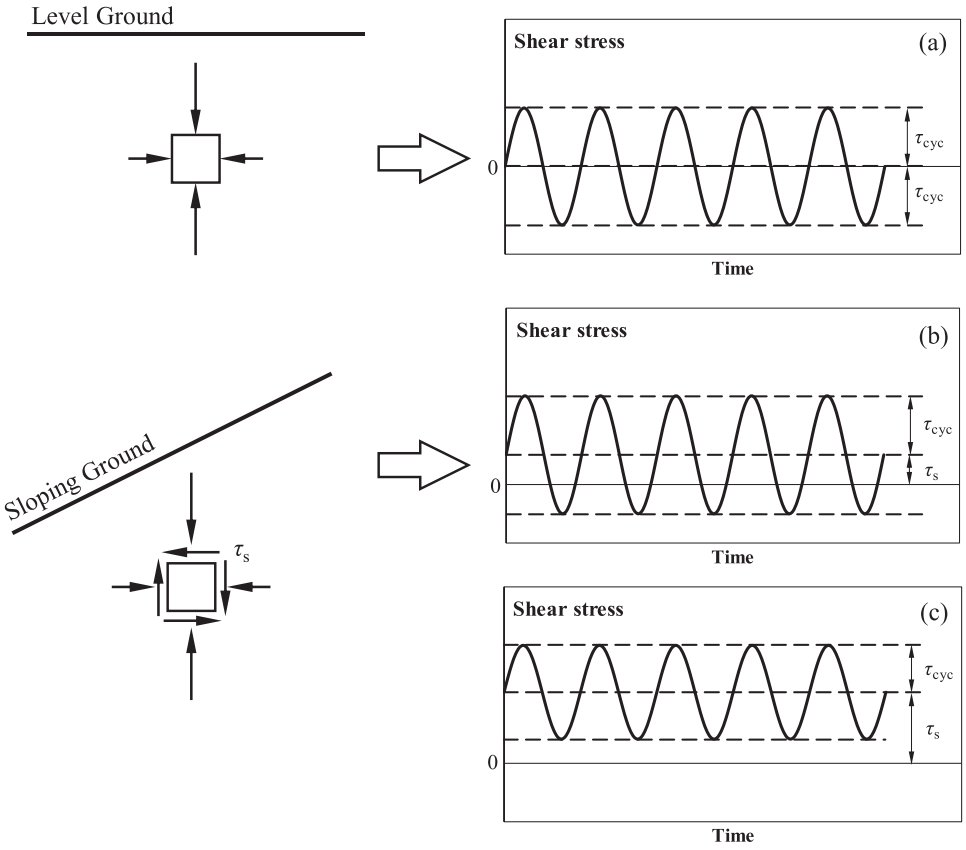

Fig. 1. Cyclic loading conditions to replicate the level ground and sloping ground conditions: (a) level ground symmetric loading; (b) sloping ground non-symmetric loading with stress reversal; (c) sloping ground non-symmetric loading without stress reversal.

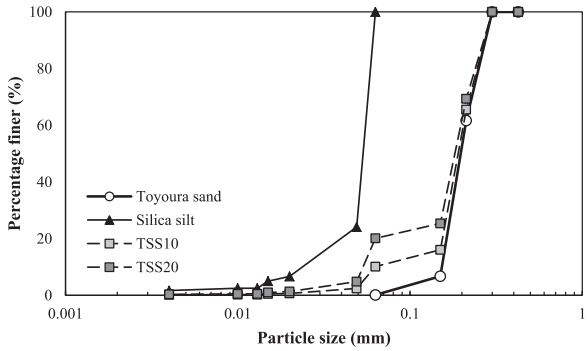

Fig. 2. Particle size distribution curves of test materials.

proposed a new platform on which the correlations between cyclic resistance and the state parameter can be represented by a straight line for each α, and these *CRR-ψ* lines rotate clockwise when α increases. These findings have provided a unified and consistent framework for interpretation of the effects of initial static shear stress and for quantifying such effects for engineering practice.

Most of the early investigations considering initial static shear stress only used clean sands with fines contents (FC) lower than 5%, including the aforementioned studies by Yang and Sze [1,20]. The natural sands, however, may contain a substantial amount of fines (referred to as silty sands), whose cyclic behavior and other mechanical properties are not yet well understood. It is of particular interest to examine whether the concept of state-dependent threshold α and the *CRR-ψ* platform are valid for silty sands. Nearly all of the current literature using silty sands mainly focused on the effects of fines content on the cyclic resistance (e.g. [21–26]) without considering the effects of initial static shear stress. A recent investigation using low plastic silty sandy soils [27] considered the effects of initial static shear stress, however the combined effects of fines and initial static shear stress remain poorly understood. Wei and Yang [28] reported a preliminary investigation into the effects of initial static shear stress on the cyclic resistance of silty sands, and the results were encouraging and justified the need for further research.

This paper presents results and findings from a comprehensive experimental program which covers a reasonably wide range of packing density, initial effective confining pressure, fines content and the initial static shear stress ratio. Following Yang and Sze [1,20], analysis is conducted from the perspective of critical state theory, with particular attention to the combined effects of initial static shear stress and fines content. An important goal of the present study is to investigate the state dependence of the threshold α and the cyclic resistance ratio as applied to silty sands such that the earlier proposed unified framework can be extended to both clean and silty sands.

2. Material and test program

This study used Toyoura sand as the base sand. It is a uniform silica sand with sub-rounded to sub-angular grains, and has been widely used in liquefaction research. Non-plastic crushed silica silt was added into Toyoura sand at various fines contents (*FC*) to create silty sand samples. Using such artificial mixtures leads to well controlled soil properties and allows a systematic investigation. The silty sands are denoted by TSS with a number indicating fines content. The particle size distribution curves of the test materials are presented in Fig. 2 and the basic properties of these materials are summarized in Table 1.

Specimens (71.1 mm in diameter and 142.2 mm in height) were reconstituted by the moist tamping method with the under-compaction technique [29]. They were saturated by percolation of CO_2 and then de-aired water. Given that liquefaction resistance is sensitive to the degree of saturation [30], the specimens were subjected to back pressure saturation and the condition of full saturation was considered to be achieved at B-values greater than 0.98. In most tests the back pressure was applied at 300kPa. The specimens were anisotropically consolidated by controlling the principal effective stresses σ'_1 and σ'_3 in small increments such that a constant α level was maintained until the desired stress condition was reached. The initial static shear stress ratio, α, is defined by the following equation:

$$\alpha = \frac{q_s}{2\sigma'_{nc}} = \frac{\sigma'_{1c} - \sigma'_{3c}}{\sigma'_{1c} + \sigma'_{3c}} \quad (1)$$

where q_s is the initial static deviatoric shear stress, σ'_{nc} ($= (\sigma'_{1c} + \sigma'_{3c}) / 2$) is the effective normal stress on the maximum shear stress plane of the specimen. After consolidation, cyclic deviatoric stress with an amplitude of q_{cyc} was applied by the computer-controlled pneumatic loading system to the specimen under undrained conditions. If $q_{cyc} > q_s$, the loading is with stress reversal; otherwise, it is without stress reversal. The amplitude of the cyclic loading is characterized by the cyclic shear stress ratio (*CSR*) defined as follows:

$$CSR = \frac{q_{cyc}}{2\sigma'_{nc}} \quad (2)$$

The test series covered a range of fines contents (FC = 10% and 20%), packing density (post consolidation void ratio, $e_c \approx$ 0.920–0.717), effective confining pressure (σ'_{nc} = 40–300 kPa) and initial static shear stress ratio (α = 0–0.4). The test conditions are summarized in Table 2. As there are no standards for laboratory measurement of the maximum and minimum void ratios for sand with high fines content, and to avoid the uncertainty associated with laboratory measurement, the relative density for each specimen was not determined. Nevertheless, as shown by Yang and Wei [31] and shown in the next sections, the conventional global void ratio is a useful density index for characterizing the mechanical behavior of

Table 1
Basic properties of the tested materials.

Material	D_{50} (mm)	C_u	C_c	G_s	e_{max}	e_{min}
Toyoura sand	0.199	1.367	0.962	2.64	0.977	0.605
Crushed silica silt	0.053	2.176	1.765	2.65	–	–
TSS10	0.192	3.266	2.178	2.64	–	–
TSS20	0.185	3.700	2.293	2.64	–	–

Table 2
Undrained cyclic triaxial test program.

Material	Target void ratio	Measured void ratio (e_c)	Initial static shear stress ratio (α)	Initial effective normal stress (σ_{nc}', kPa)	Initial state parameter (ψ)	CRR_{10}	CRR_{15}
TSS10	0.910	0.912	0	100	0.036	0.134	0.123
TSS10	0.903	0.906	0	100	0.030	0.148	0.141
	0.903	0.907	0.1	100	0.030	0.190	0.177
	0.903	0.906	0.15	100	0.029	0.209	0.194
	0.903	0.908	0.2	100	0.030	0.220	0.206
	0.903	0.904	0.25	100	0.026	0.212	0.199
	0.903	0.907	0.4	100	0.029	0.172	0.152
TSS10	0.903	0.903	0	300	0.060	0.118	0.111
	0.903	0.905	0.1	300	0.061	0.152	0.140
	0.903	0.904	0.25	300	0.057	0.084	0.078
	0.903	0.903	0.4	300	0.054	0.003	0
TSS10	0.847	0.849	0	100	−0.027	0.179	0.172
	0.847	0.848	0.1	100	−0.029	0.227	0.215
	0.847	0.850	0.25	100	−0.028	0.279	0.271
	0.847	0.852	0.4	100	−0.027	0.304	0.274
TSS10	0.791	0.791	0	40	−0.100	0.323	0.291
	0.791	0.790	0.25	40	−0.102	0.459	0.422
	0.791	0.790	0.4	40	−0.103	0.550	0.517
TSS10	0.791	0.795	0	100	−0.081	0.269	0.248
	0.791	0.792	0.1	100	−0.085	0.322	0.302
	0.791	0.793	0.25	100	−0.085	0.402	0.372
	0.791	0.795	0.4	100	−0.084	0.482	0.441
TSS10	0.791	0.794	0	300	−0.049	0.205	0.193
	0.791	0.793	0.1	300	−0.051	0.259	0.244
	0.791	0.793	0.25	300	−0.054	0.305	0.287
	0.791	0.794	0.4	300	−0.054	0.371	0.352
TSS10	0.717	0.722	0	100	−0.154	0.422	0.378
TSS20	0.920	0.917	0	100	0.090	0.080	0.073
TSS20	0.903	0.906	0	100	0.079	0.110	0.104
	0.903	0.906	0.1	100	0.078	0.136	0.125
	0.903	0.907	0.25	100	0.078	0.096	0.090
	0.903	0.904	0.35	100	0.074	0.047	0.044
TSS20	0.791	0.790	0	40	−0.053	0.240	0.227
	0.791	0.790	0.25	40	−0.055	0.391	0.366
	0.791	0.790	0.4	40	−0.055	0.469	0.452
TSS20	0.791	0.795	0	100	−0.032	0.204	0.190
	0.791	0.795	0.1	100	−0.033	0.254	0.233
	0.791	0.794	0.25	100	−0.035	0.333	0.312
	0.791	0.796	0.4	100	−0.034	0.412	0.400
TSS20	0.791	0.791	0	300	0.000	0.162	0.152
	0.791	0.795	0.1	300	0.002	0.199	0.185
	0.791	0.794	0.25	300	−0.001	0.238	0.226
	0.791	0.796	0.4	300	−0.001	0.190	0.179
TSS20	0.717	0.719	0	100	−0.108	0.311	0.284

silty sands, particularly in the framework of critical state soil mechanics.

3. Cyclic failure patterns

Sze and Yang [32] reported three distinctly different failure patterns of reconstituted clean sand, known as flow-type failure, cyclic mobility and plastic strain accumulation. Which failure pattern will occur depends on several factors such as packing density, initial effective confining pressure, stress reversal condition, and reconstitution method. These failure patterns are also typical for non-plastic silty sands tested in the present study.

Fig. 3 illustrates the cyclic behavior of loose TSS10 ($e_c \approx 0.903$, $\sigma'_{nc} = 100$ kPa). For loose specimens, the flow type failure or the runaway deformation was found to be the unique failure patterns regardless of α. The presence of initial static shear stress and the stress reversal condition only influenced the direction of axial strain development. The excess pore water pressure gradually increased with loading cycles, but the axial strain development was small ($\varepsilon_a < 5\%$). When the excess pore water pressure reached a certain point it increased suddenly and dramatically, accompanied by an abrupt development of large deformation. If such flow-type failure occurs in situ, it may cause catastrophic consequences because of its sudden nature.

Fig. 4 presents the cyclic response of TSS10 in a relatively dense

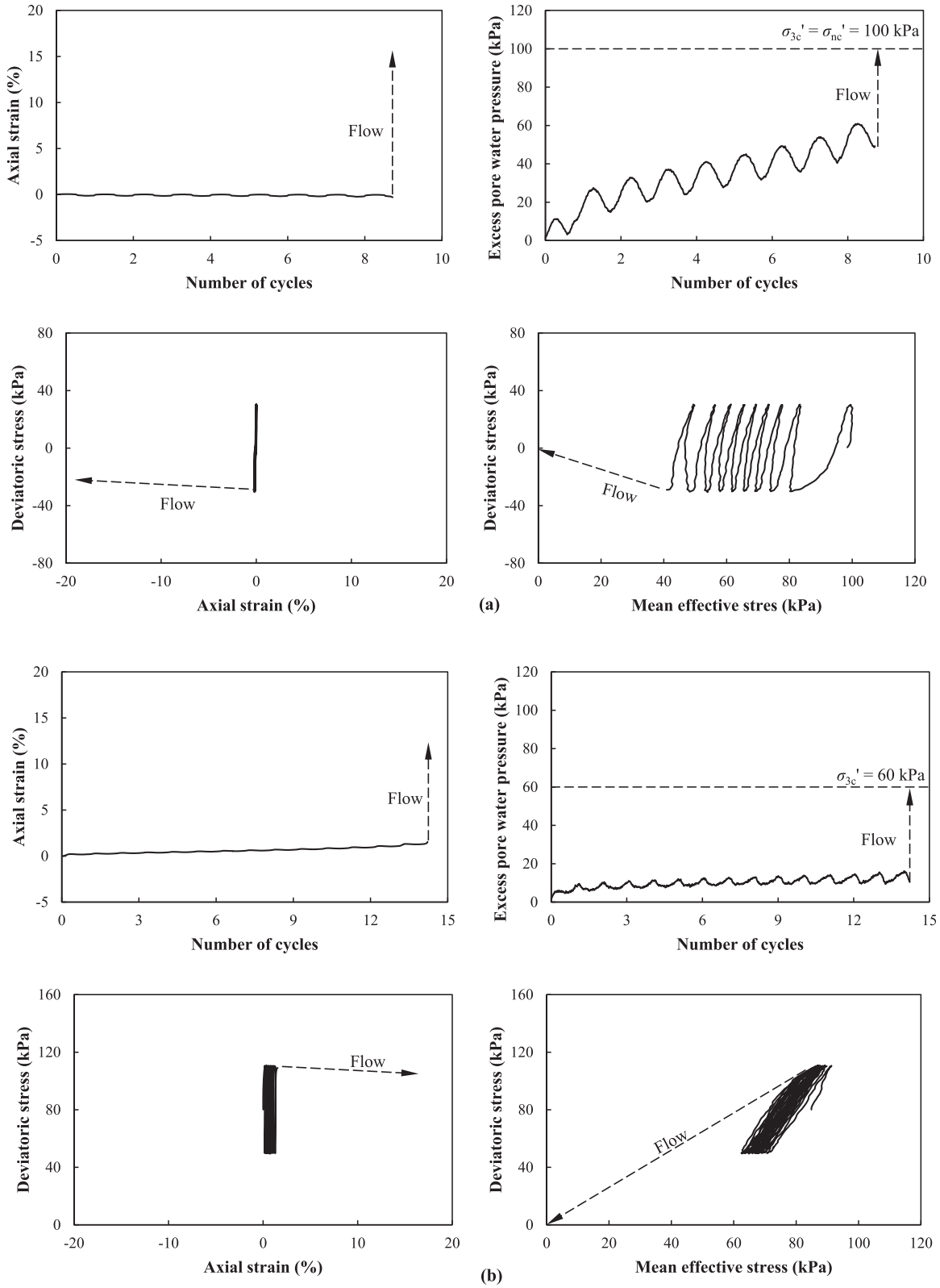

Fig. 3. (a): Cyclic response of silty sand (flow-type failure): TSS10, $e_c = 0.903$, $\sigma_{nc}' = 100$kPa, $\alpha = 0$, $CSR = 0.15$. (b): Cyclic response of silty sand (flow-type failure): TSS10, $e_c = 0.908$, $\sigma_{nc}' = 100$kPa, $\alpha = 0.4$, $CSR = 0.15$.

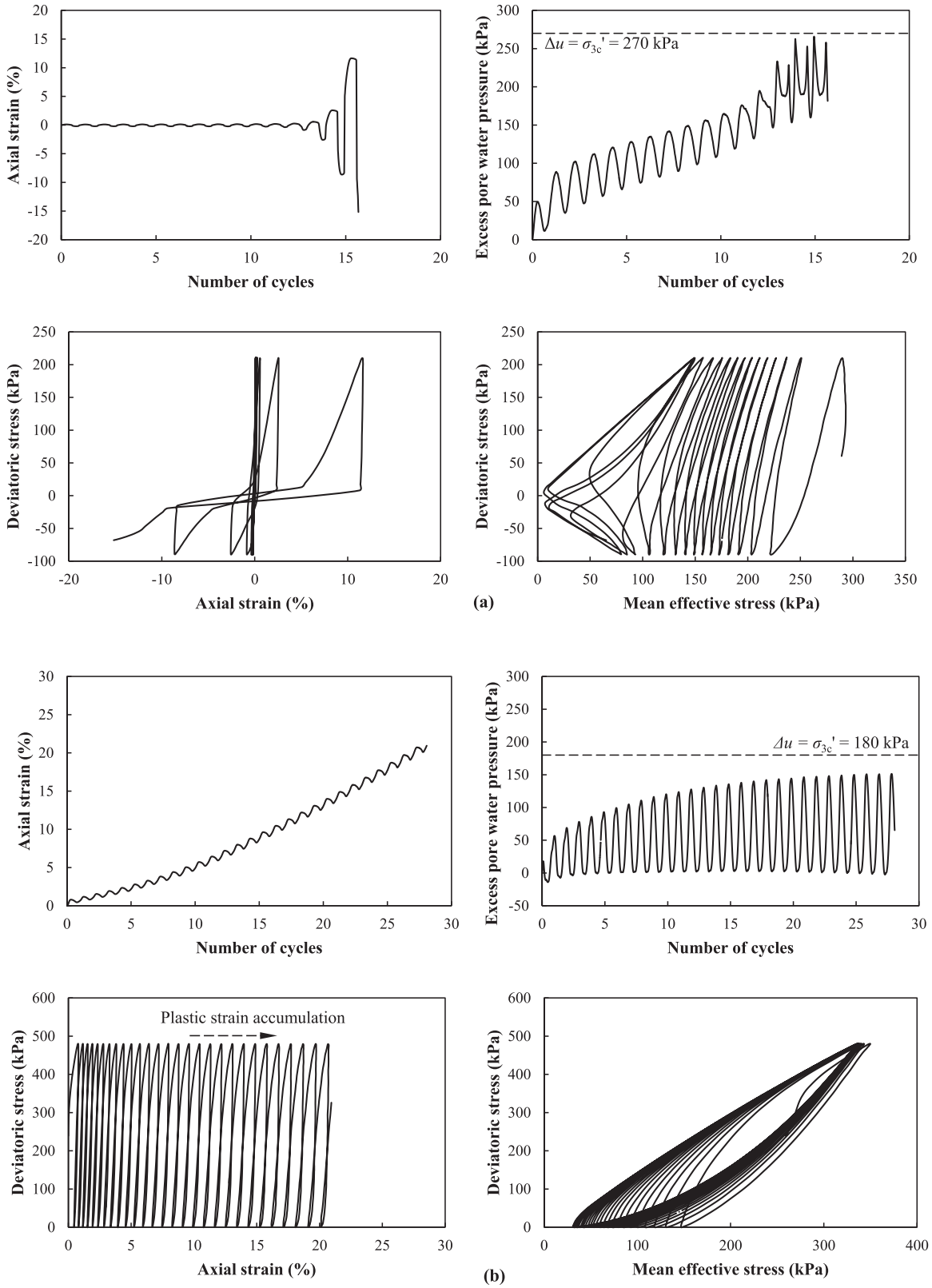

Fig. 4. (a): Cyclic response of silty sand (cyclic mobility): TSS10, e_c = 0.795, σ_{nc}' = 300kPa, α = 0.1, CSR = 0.25. (b): Cyclic response of silty sand (plastic strain accumulation): TSS10, e_c = 0.793, σ_{nc}' = 300kPa, α = 0.4, CSR = 0.4.

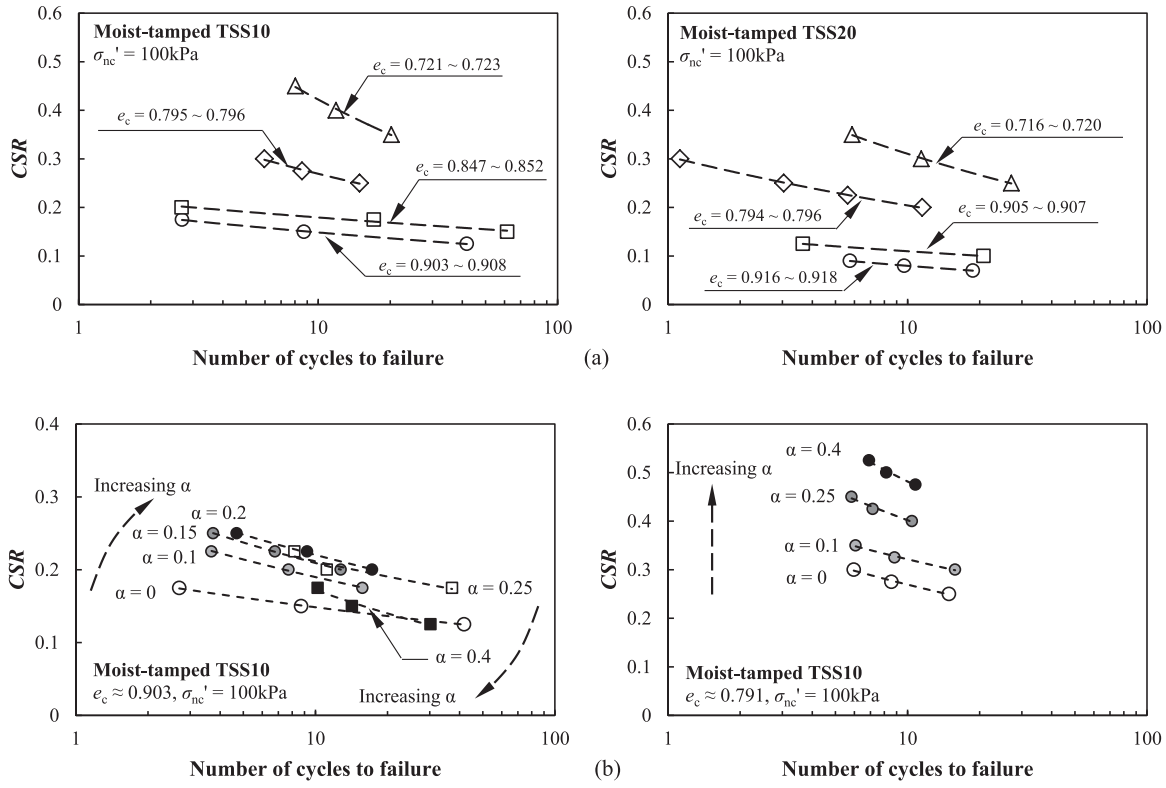

Fig. 5. *CSR*-N_l relationships: (a) $\alpha = 0$; (b) $\alpha \neq 0$.

state ($e_c \approx 0.791$, $\sigma'_{nc} = 300$kPa) with the presence of initial static shear stress, but under different stress reversal conditions. Fig. 4(a) illustrates a typical failure pattern known as cyclic mobility which occurs in medium dense to dense specimens loaded under reversed stress conditions ($CSR > \alpha$). The excess pore water pressure increased gradually with loading cycles and finally reached a transient liquefied state ($\Delta u = \sigma'_{nc}$, $p' = 0$). The first transient liquefied state is commonly named initial liquefaction and subsequent liquefied states occur when the cyclic stress reverses its direction. The axial strain developed in a cyclic pattern during loading cycles before initial liquefaction. Large deformation occurred during the loading cycles after the initial liquefaction, when the direction of deviatoric stress reversed. The large deformation is associated with the transient liquefied state, where the effective stress is almost zero and the stiffness of the soil is rather low. Because the liquefied states are transient, the soil did not collapse but regained its strength and stiffness due to dilation when the soil was continuously loaded. As the number of loading cycles increased, such behavior repeated and the double amplitude (DA) of axial strain accumulated until a very large value was reached. Such failure behavior leads to severe serviceability problem if it occurs in situ. The initial static shear stress may cause the strain development more biased on the compression side.

The plastic strain accumulation is a typical failure pattern for medium dense to dense specimens loaded without stress reversal (Fig. 4(b)). Irrecoverable axial strain accumulated on the compression side ($\varepsilon_a > 0$) as the cyclic stress remained purely compressional ($CSR = \alpha$). The excess pore water pressure increased cyclically, but never equaled to the initial lateral confining pressure (σ'_{3c}). This behavior implies that the accumulation of plastic deformation controls failure of the specimen rather than the pore water pressure generation [1]

4. Cyclic resistance

Yang and Sze [1] proposed consistent failure criteria for estimating the cyclic resistance of Toyoura sand, based on different failure patterns. Apparently, these criteria are applicable for the silty sands in the present study. For sands exhibiting flow-type failure, the onset of flow is used to define failure. For cyclic mobility, the attainment of 5% DA axial strain is defined as failure. For plastic strain accumulation, the failure is defined as the attainment of 5% peak axial strain. Different *CSR*s were applied to replicated specimens, resulting in different numbers of cycles to failure (N_l). Selected *CSR*-N_l relationships are presented in Fig. 5. Nearly all the *CSR*-N_l plots cover data points for $N_l = 10$ or close. Therefore, the cyclic resistance ratio (*CRR*) is characterized here by the *CSR* causing failure in 10 cycles in accordance with Yang and Sze [1].

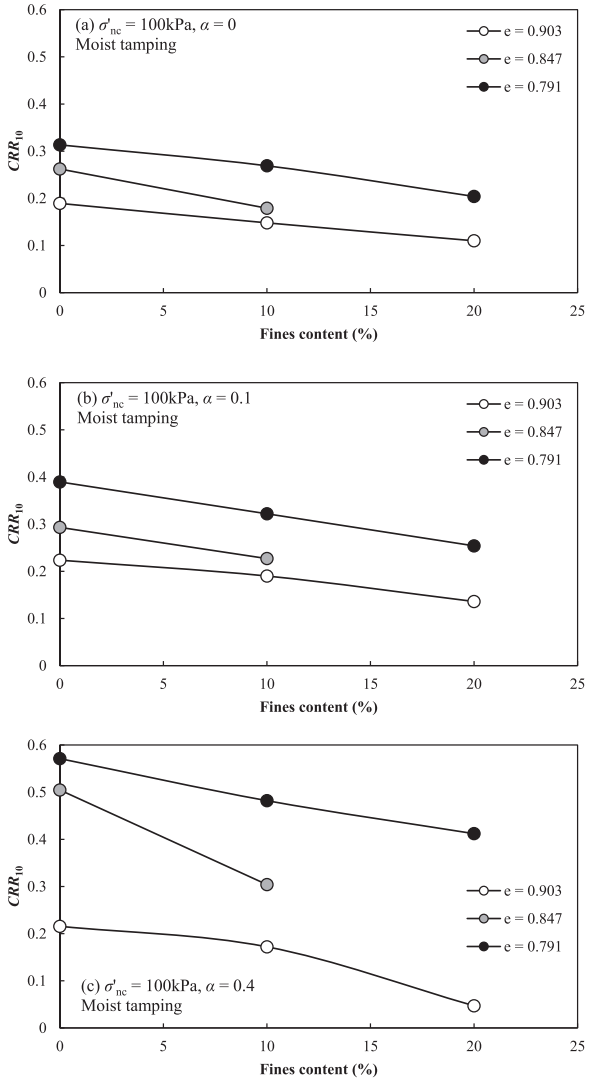

Fig. 6. Effects of fines content on the cyclic resistance of silty sands (clean sand data from Yang and Sze [1,20]).

4.1. Effects of fines

When the fines content is lower than the threshold fines content (FC_{th}), i.e. the fines content separating the sand-dominant and fines-dominant structure, literature data showed that addition of non-plastic fines could reduce the cyclic resistance when compared at the same void ratio for cases where $\alpha = 0$. The test results in Fig. 6(a) confirmed this observation for $FC < FC_{th}$, given that $FC_{th} = 40\%$ according to Yang and Wei [31]. The effects of fines were rarely reported for cases with initial static shear stress in the literature. The present study investigated the two factors collectively and the results are presented in Fig. 6(b) and (c), showing that addition of crushed silica silts decreases *CRR* for specimens with the presence of initial static shear stress. This figure only presents the test results under σ_{nc}' = 100 kPa. For other initial confining pressure levels, similar results can be observed.

4.2. Effects of packing density

As shown in Fig. 7, the cyclic resistance of silty sands decreases with increasing void ratio and the *CRR-e* trend lines shift downwards with increasing fines content for all α levels. In addition, the sensitivity of *CRR* to the void ratio is affected by α, if the data in Fig. 7 are compared for the same material. The *CRR* decreased more significantly with a certain increment of void ratio for higher α values (e.g. $\alpha = 0.4$) than for lower α values (e.g. $\alpha = 0.1$). These observations are made on test data under $\sigma'_{nc} = 100$ kPa. As will be shown later, the initial effective confining pressure can also affect the cyclic resistance of silty sands.

4.3. Effects of confining pressure

The effects of initial effective stress can be observed in Fig. 8. Clearly the cyclic resistance decreases with increasing initial confining pressure level for all fines contents and α levels. The initial effective confining pressure is an important parameter that cannot be ignored when characterizing cyclic resistance. In addition, the effects of confining pressure on CRR are also affected by fines content and initial static shear stress. The *CRR*-σ'_{nc} curves shift downwards with increasing fines content. The curves for lower α values (e.g. $\alpha = 0$) are more or less parallel with each other for different fines contents. When α value is relatively higher (e.g. $\alpha = 0.4$), the gradient of the *CRR*-σ_{nc}' curve becomes more sensitive to the fines content, i.e. *CRR* decreases more significantly with initial effective stress for higher fines content and higher α levels.

4.4. Effects of initial static shear stress

Yang and Sze [1,20] reported that the effects of α on the cyclic resistance of clean sands can be either beneficial or detrimental mainly depended on initial packing density and the initial effective confining pressure. Similar observations can be found for silty sands tested in the present study. Fig. 9(a) shows the effects of initial void ratio on the *CRR*-α relationship for TS, TSS10 and TSS20. The effects of α can be positive when the void ratio is relatively lower (e.g. $e_c = 0.791$ for both TSS10 and TSS20). Whereas, for a relatively larger void ratio (e.g. $e_c = 0.903$) the effects of α can be firstly positive and then become negative after a certain value. According to Yang and Sze [1], the no-reversal line, representing *CRR* = α, may serve as a boundary dividing such positive and negative effects. The impact of initial confining pressure on the effects of α is shown in Fig. 9(b). For the case of TS with $e_c \approx 0.903$, the increase of σ'_{nc} from 100 to 500 kPa decreases *CRR* and leads to a more significant reduction of *CRR* for $\alpha >$ *CRR* when α increases. For the case of TSS10 with $e_c \approx 0.791$, the effective confining pressure only decreases the cyclic resistance, leading to nearly parallel *CRR*-α curves. For the case of TSS20 with $e_c \approx 0.791$, the *CRR*-α curves show a positive effect of α and are parallel on the left side of the no-reversal line when the confining pressure increases from 40 kPa to 100 kPa; whereas the *CRR* starts to decrease after the *CRR*-α curve crosses the no-reversal line when the pressure increases to 300 kPa.

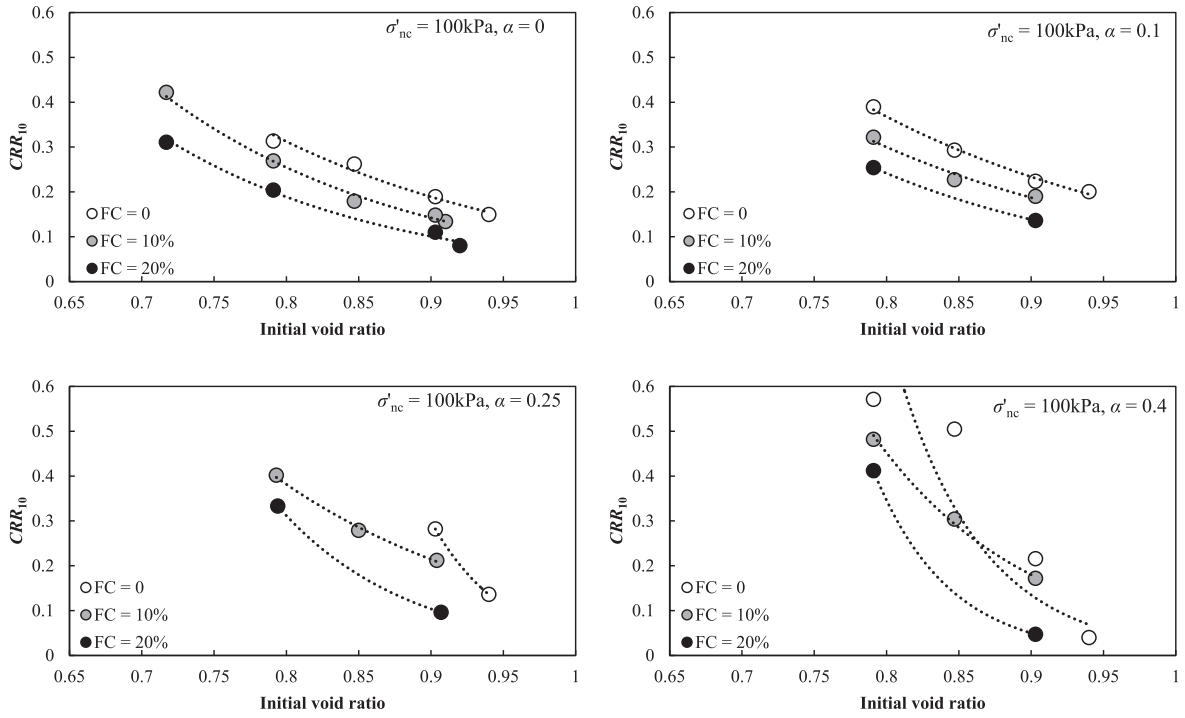

Fig. 7. Effects of packing density on cyclic resistance of silty sands for various *FC* and α (clean sand data from Yang and Sze [1,20]).

To characterize the effect of α, an initial static shear correction factor, K_α, was introduced by Seed [9]. It is defined as follows.

$$K_\alpha = \frac{CRR_{\alpha\neq 0}}{CRR_{\alpha=0}} \tag{3}$$

where $CRR_{\alpha\neq 0}$ and $CRR_{\alpha=0}$ are cyclic resistance ratio under different α values but the same initial packing density and effective confining pressure. The impact of initial void ratio is presented in Fig. 10(a), whereas the impact of confining pressure is presented in Fig. 10(b). The K_α-α relationships almost coincide with each other when K_α increases with α, and then deviate when α has negative effects for some initial states.

Importantly, the cases of TS and TSS20 shown in Fig. 10(b) provide solid evidence that the effects of initial confining pressure cannot be ignored, even when $\sigma'_{nc} < 300$ kPa. For the TS case, all the K_α-α curves first increase in a very similar way and then decrease in different gradients. K_α decreases more significantly with increasing α if the effective confining pressure is higher. For the TSS20 case, the K_α-α curve for 300 kPa slightly deviates from the other two (40 kPa and 100 kPa) for α values between 0.1 and 0.25. And the difference becomes rather significant when $\alpha = 0.4$. Thus, for both the clean and silty sands, the effects of confining pressure on the K_α-α relationship can be significant when α exerts a negative impact. Such negative effect occurs more commonly in relatively loose states. This may partly explain the large scatter observed in the Harder and Boulanger's proposal [6] which ignored the effects of effective overburden pressure.

5. Critical-state-based analysis

The analysis in the previous section indicates that *CRR* is a function of several factors including packing density, effective confining pressure, fines content and initial static shear stress. However, characterization of their effects on *CRR* is not easy because the impact of a certain factor can be affected by the remaining factors. The critical state theory has been found useful to characterize the liquefaction resistance and other mechanical behaviors of sands [1,20,33,34]. Fig. 11 shows the critical state lines (CSL) of the clean Toyoura sand [35] and the two silty sands [36] determined from undrained monotonic tests. These CSLs are formulated using the following equation.

$$e_{CS} = e_\Gamma - \lambda_c\left(\frac{p'}{P_a}\right)^{0.6} \tag{4}$$

where e_Γ and λ_c are parameters of the CSL which can be affected by the fines content; P_a is a reference pressure equaling to atmospheric pressure. The positions of CSLs are controlled by e_Γ, which decreases with increasing *FC*, as shown in Fig. 11. The concept of state parameter, ψ, proposed by Been and Jefferies [19], was found useful to characterize the cyclic resistance and other mechanical behavior of sands. It is defined as the vertical distance between the initial state (in terms of void ratio and mean effective stress prior to shearing) and the CSL. A lower value of ψ indicates a more dilative behavior than a higher value of ψ.

When the effect of *FC* on cyclic resistance is examined the other factors need to be controlled. In other words, the initial state in terms of

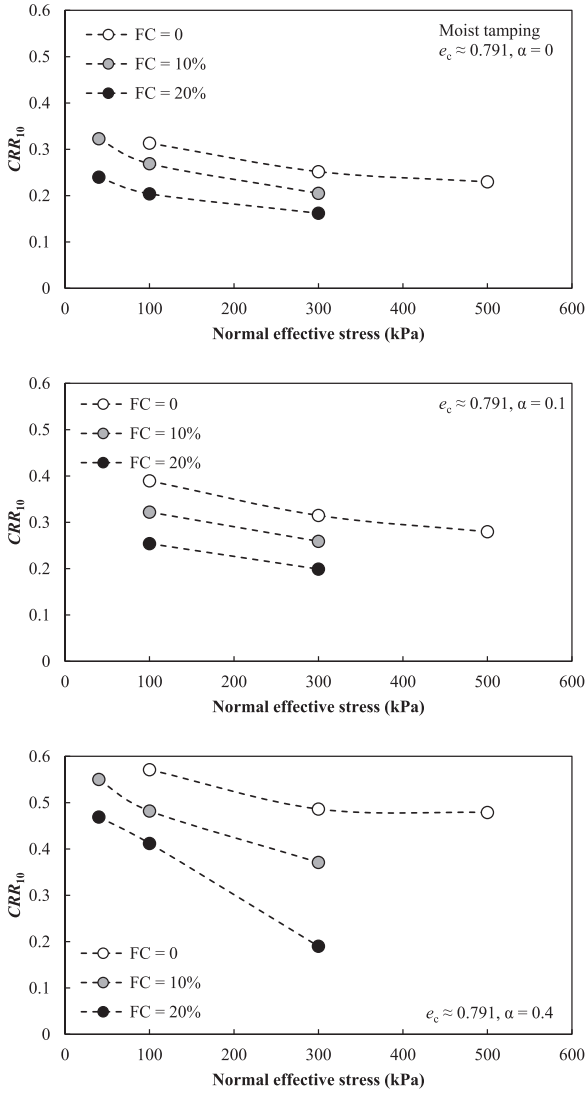

Fig. 8. Effects of confining pressure on cyclic resistance of silty sands for various *FC* and *α* (clean sand data from Yang and Sze [1,20]).

void ratio and mean effective stress should be similar for sands with different *FCs*. Because of different positions of the CSLs due to different *FCs*, the initial state parameter of the three sands are different (Fig. 11(a)), with TSS20 having the highest state parameter whereas TS having the lowest. The higher the initial state parameter, the more contractive is the behavior. This means a faster build-up of excess pore water pressure and thus a lower cyclic resistance should be expected. Similarly, decreasing e_c and decreasing σ'_{nc} (Fig. 11(b) and (c)) will lead to lower state parameters and thus more dilative response with higher cyclic resistance.

5.1. FC-unified CRR-ψ correlations

Under the framework of critical state soil mechanics, Yang and Sze [20] characterized *CRR* of clean Toyoura sand for each initial shear stress level and proposed the *CRR*-*ψ* platform. In that platform the effects of packing density and confining pressure are unified by a *CRR*-*ψ* correlation which can be characterized fairly well by a linear trend line for a given *α* level. These trend lines rotate clockwise with increasing *α*, as shown in Fig. 12(a). The *CRR*-*ψ* data of the two silty sands are plotted to compare with the trend lines calibrated by clean sand data in Fig. 12(b). The new data of silty sands fall into the vicinity of the trend lines, implying that the correlation is FC-unified. In addition, it is found that the *α*-induced clockwise rotation of the *CRR*-*ψ* curves is also applicable to silty sands.

5.2. Threshold α for silty sands

The threshold *α* values are determined for silty sands by intersecting the no-reversal line and the *CRR*-*α* curve. Values of threshold *α* for silty sands are obtained and compared with those for clean sands. The results in Fig. 13 indicate that increasing fines content can decrease the value of α_{th} under otherwise similar conditions. The effect of *FC* on α_{th} is the same on *CRR*. In fact, there are many similarities between α_{th} and *CRR* because α_{th} corresponds to the maximum *CRR* at a certain initial state in terms of packing density and initial effective confining pressure.

The state dependency of α_{th} has been proposed by Yang and Sze [1], which can be expressed by a linear α_{th}-*ψ* relationship. The correlation between the *CRR*-*ψ* relationship and the α_{th}-*ψ* relationship has been interpreted by Yang and Sze [20]. Given the FC-unified *CRR*-*ψ* for silty sand in this study, it is interesting to compare the α_{th}-*ψ* of the silty sands with that of the clean sand in Fig. 14. Based on test data on clean sand, Yang and Sze [1] proposed the following equation to characterize the α_{th}-*ψ* relationship:

$$\alpha_{th} = -2.085\psi + 0.221 \quad (5)$$

This relationship is plotted in Fig. 14 to compare with the new data on two silty sands. Apparently, the new data fall into the vicinity of the trend line. Using both clean and silty sand data, an improved relationship can be given as follows:

$$\alpha_{th} = -1.593\psi + 0.222 \quad (6)$$

6. Discussions

The obvious advantage of the *CRR*-*ψ* platform is that it unifies the effects of packing density, effective confining pressure and fines content in the framework of critical state soil mechanics. Moreover, the effects of initial static shear stress can be isolated on this platform and be characterized by the clockwise rotation of the *CRR*-*ψ* curves. Given these attractive advantages, it is worthwhile to extend the study to address several remaining issues in future. The first one is about the effects of fabric. In this study, the proposed *CRR*-*ψ* and α_{th}-*ψ* correlations are based on specimens reconstituted by the moist-tamping method. The cyclic resistance can be affected by different sample preparation methods or different initial fabrics of sand samples (e.g. Sze and Yang [32]). The second issue is on the effect of particle characteristics. Several recent studies [32,37,38] have shown solid evidence that the mechanical behavior of sands is highly affected by such factors as particle shape and gradation. Thus, it is of interest to study the applicability of the proposed framework on soils with different soil

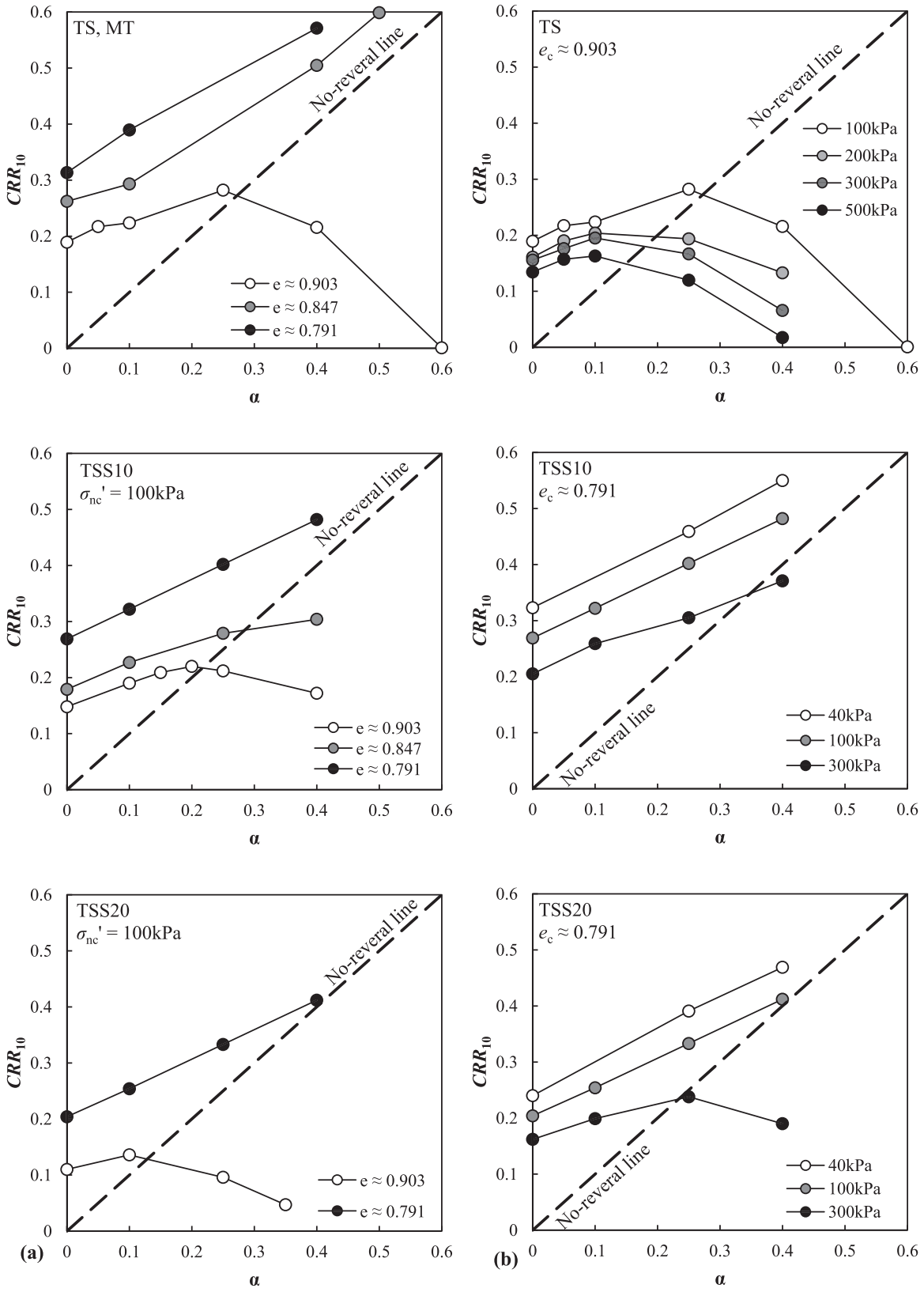

Fig. 9. (a): Effects of *α* on *CRR* for various packing density. (b): Effects of *α* on *CRR* for various confining pressure.

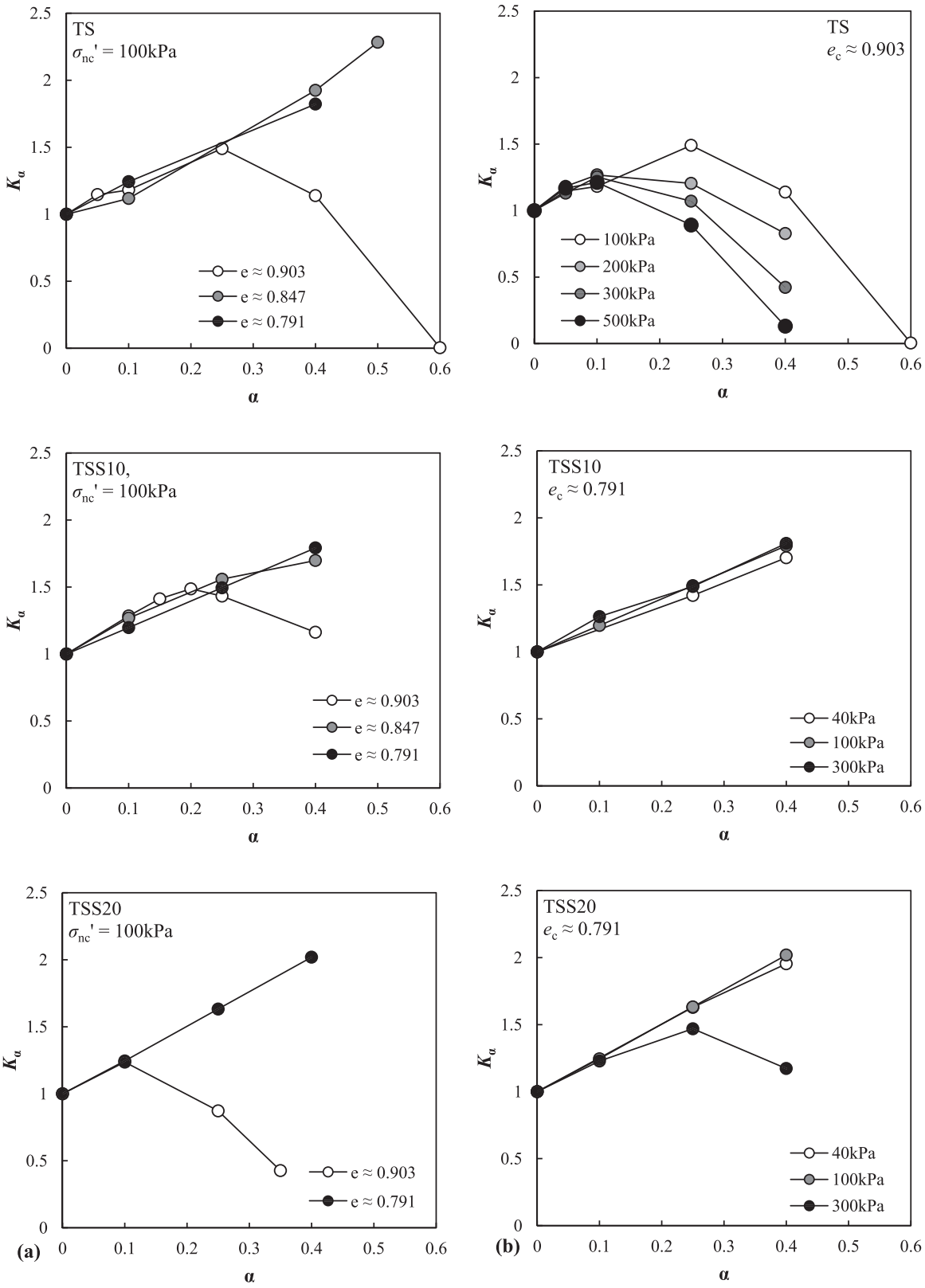

Fig. 10. (a): K_α-α relationships considering the effects of packing density. (b): K_α-α relationships considering the effects of confining pressure.

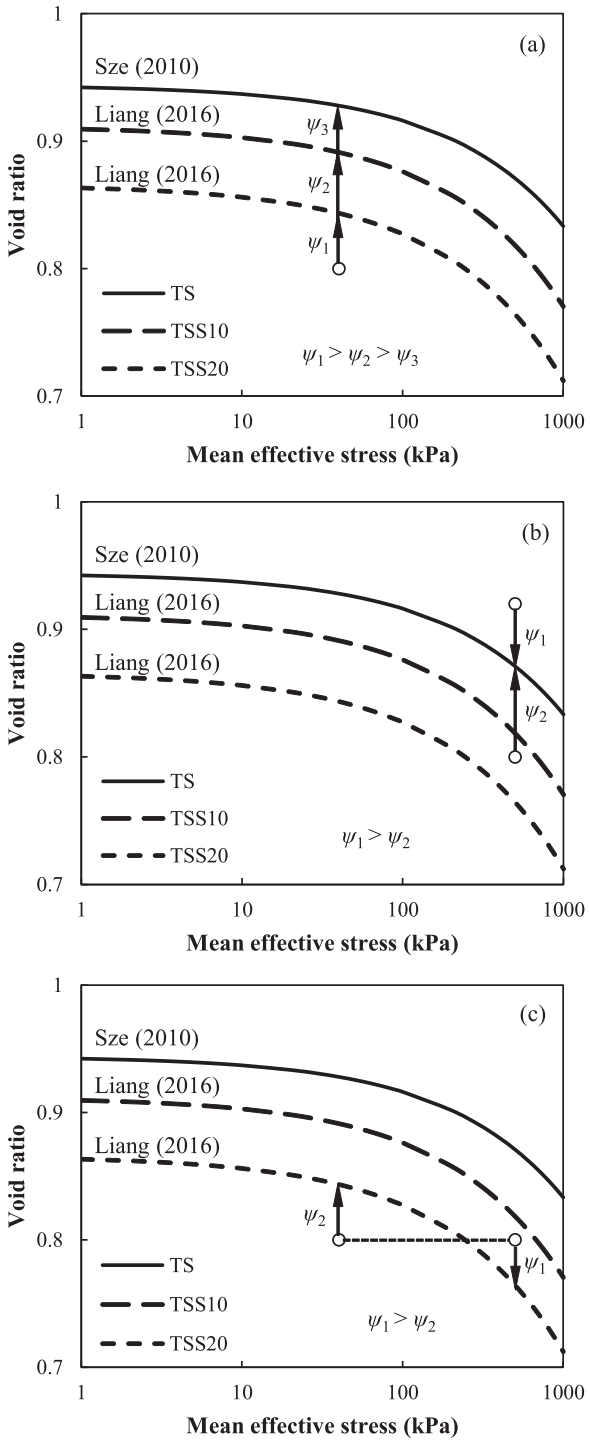

Fig. 11. Critical state lines of tested materials and factors affecting the initial state parameter of the materials: (a) effect of FC, (b) effect of initial packing density, and (c) effect of initial effective confining pressure.

properties. The third one is the effect of preloading history. Wichtmann et al. [39] reported strong correlation between drained cyclic preloading and liquefaction resistance. Future investigation of the preloading effect in the proposed framework would be of interest. The fourth one is the cyclic stress path introduced by different loading conditions. It has been observed that cyclic simple shear condition usually resulted in a lower cyclic resistance than the cyclic triaxial condition [40,41]. There have been several studies on the effects of initial static shear stress under cyclic simple shear condition, but none of these data was analyzed in the proposed framework. Future work along the line would be of interest.

Additionally, it is worth mentioning that several studies in the literature proposed to use an equivalent skeleton void ratio as the density index for silty sands (e.g. [42]). While it appears to be interesting, the rationale behind the equivalent skeleton void ratio, particularly the physical meaning of the parameter *b* involved in the definition, remains open for discussion. The global void ratio remains a useful density index for characterizing the mechanical behavior of silty sands especially in the framework of critical state soil mechanics, as shown in this paper and in previous papers [31,34]. Detailed discussion about this point can be referred to Yang et al. [43] and Luo and Yang [44].

7. Conclusions

This paper has presented results and findings from a systematic testing program to investigate the cyclic behavior and liquefaction resistance of silty sands with the presence of initial static shear stress. The laboratory tests covered a reasonably wide range of packing density, effective confining pressure and initial static shear stress ratio, and the range of fines content (FC) was between 0% and 20% such that all silty sand specimens can be assumed to be sand-dominated. The cyclic resistance of the silty sands has been characterized in the framework of critical state soil mechanics. The main conclusions can be drawn as follows.

1. When compared at the same initial void ratio and effective confining pressure, the addition of crushed silica silt reduces the cyclic resistance (*CRR*) of silty sands for all initial shear stress levels (i.e. α levels).
2. The cyclic resistance of silty sands depends on the initial packing density and the initial effective confining pressure. Similar to clean sand, the cyclic resistance of silty sand decreases with increasing initial void ratio and initial effective confining pressure, and vice versa. But the presence of an initial static shear stress can affect the effects of void ratio and confining pressure on cyclic resistance.
3. The effects of α on cyclic resistance can be beneficial or detrimental depending on the initial packing density and the initial confining pressure. The concept of threshold α, originally developed for clean sand, can also be applied to silty sands. The threshold α is affected by the initial packing density and initial effective confining pressure.
4. The cyclic resistance of silty sands can be characterized by the initial state parameter ψ. Unified correlations between *CRR* and ψ can be obtained for different fines contents at a given α level. The *CRR*-ψ lines rotate clockwise with increasing α. The threshold α can also be characterized for various fines contents by using the initial state parameter.

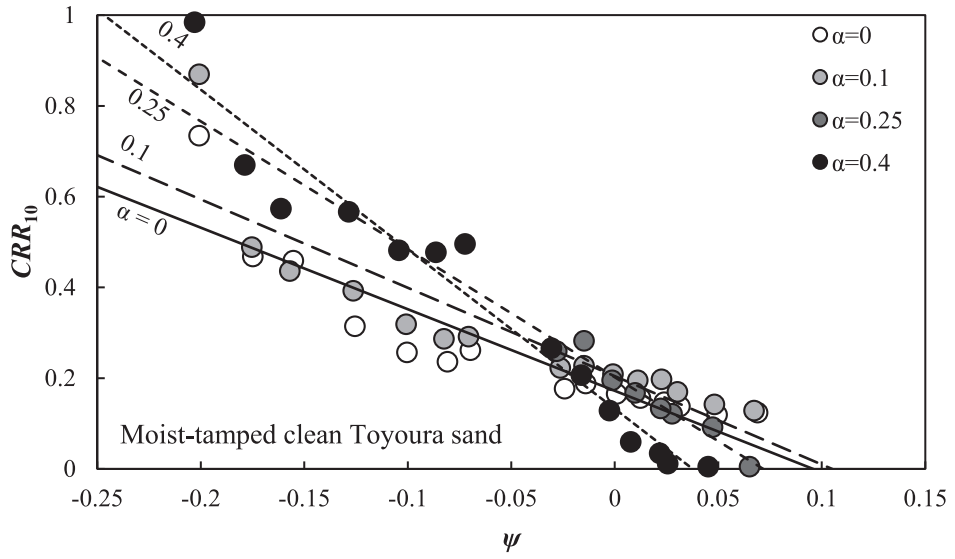

(a) *CRR*-ψ of clean Toyoura sand under different α levels (Yang & Sze [1,20])

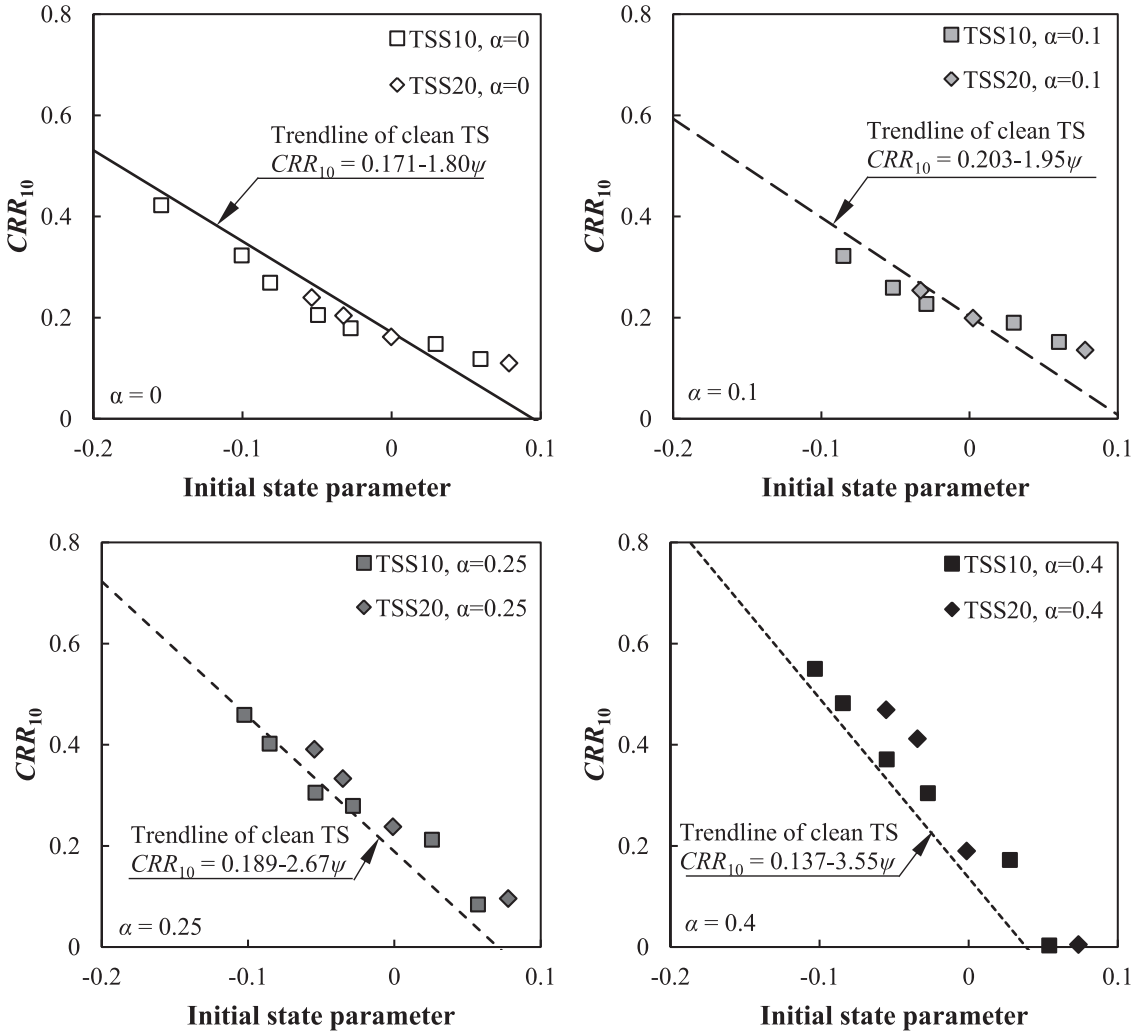

(b) *CRR*-ψ of Toyoura sand with fines under different α levels

Fig. 12. Clockwise rotation of the *FC*-unified *CRR*-ψ correlations.

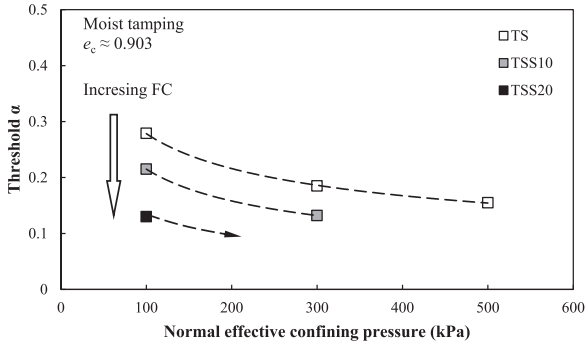

Fig. 13. Threshold α determined for clean and silty sands.

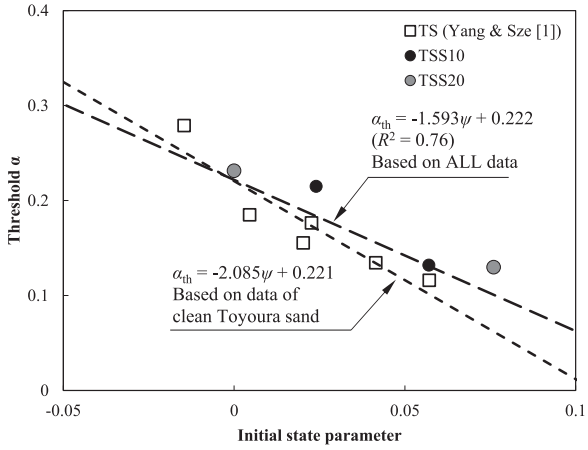

Fig. 14. FC-unified α_{th}-ψ correlation.

5. The unified *CRR*-ψ platform together with the unified α_{th}-ψ correlation suggests that the cyclic resistance of both clean and non-plastic silty sands can be consistently characterized, thus providing an attractive, unified framework for understanding the effects of initial static shear stress on soil liquefaction and for quantifying such effects for engineering practice.

Acknowledgements

The financial support provided by the Research Grants Council of Hong Kong (Nos. 17250316; 17206418) and by the MOE Key Laboratory of Soft Soils and Geoenvironmental Engineering of Zhejiang University (No. 2018P02) is acknowledged.

References

[1] Yang J, Sze HY. Cyclic behaviour and resistance of saturated sand under non-symmetrical loading conditions. Géotechnique 2011;61(1):59–73.
[2] Toki S, Tatsuoka F, Miura S, Yoshimi Y, Yasuda S, Makihara Y. Cyclic undrained triaxial strength of sand by a cooperative test program. Soils Found 1986;26(3):117–28.
[3] Seed HB. Soil liquefaction and cyclic mobility evaluation for level ground during earthquakes. J Geotech Eng Div 1979;105(2):201–55.
[4] Hyodo M, Orense RP, Noda S, Furukawa S, Furui T. Slope failures in residential land on valley fills in Yamamoto town. Soils Found 2012;52(5):975–86.
[5] Vaid YP, Stedman JD, Sivathayalan S. Confining stress and static shear effects in cyclic liquefaction. Can Geotech J 2001;38(3):580–91.
[6] Harder Jr LF, Boulanger R. Application of K_σ and K_α correction factors. In: Proceedings of NCEER workshop on evaluation of liquefaction resistance of soils, State University of New York at Buffalo; 1997.
[7] Yoshimi Y, Oh-Oka H. Influence of degree of shear stress reversal on the liquefaction potential of saturated sand. Soils Found 1975;15(3):27–40.
[8] Rollins Kyle M, Seed HB. Influence of buildings on potential liquefaction damage. J Geotech Eng 1990;116(2):165–85.
[9] Seed HB. Earthquake-resistant design of earth dams. In: Proceedings of international conferences on recent advances in geotechnical earthquake engineering and soil dynamics. St. Louis, Missouri, USA; 1981.
[10] Vaid YP, Chern JC. Cyclic and monotonic undrained response of saturated sands. in: Proceedings of advances in the art of testing soils under cyclic conditions. Detroit, Michigan, United States; 1985.
[11] Mohamad R, Dobry R. Undrained monotonic and cyclic triaxial strength of sand. J Geotech Eng 1986;112(10):941–58.
[12] Hyodo M, Tanimizu H, Yasufuku N, Murata H. Undrained cyclic and monotonic triaxial behaviour of saturated loose sand. Soils Found 1994;34(1):19–32.
[13] Seed RB, Harder Jr LF. SPT-based analysis of cyclic pore pressure generation and undrained residual strength. In: Proceedings of H. Bolton Seed Memorial Symp, Vancouver; 1990.
[14] Youd T, Idriss I, Andrus R, Arango I, Castro G, Christian J, Dobry R, Finn W, Harder LJ, Hynes M, Ishihara K, Koester J, Liao S, Marcuson III W, Martin G, Mitchell J, Moriwaki Y, Power M, Robertson P, Seed R, Stokoe II K. Liquefaction resistance of soils: summary report from the 1996 NCEER and 1998 NCEER/NSF workshops on evaluation of liquefaction resistance of soils. J Geotech Geoenviron Eng 2001;127(10):817–33.
[15] Tatsuoka F, Muramatsu M, Sasaki T. Cyclic undrained stress-strain behaviour of dense sand by torsional simple shear. Soils Found 1982;22(2):55–70.
[16] Vaid YP, Chern JC. Effect of static shear on resistance to liquefaction. Soils Found 1983;23(1):47–60.
[17] Pillai VS, Stewart RA. Evaluation of liquefaction potential of foundation soils at Duncan Dam. Can Geotech J 1994;31(6):951–66.
[18] Sivathayalan S, Ha D. Effect of initial stress state on the cyclic simple shear behaviour of sands. In: Proceedings of the international conference on cyclic behaviour of soils and liquefaction phenomena, CBS04, Bochum, Germany; 2004. p. 207–14.
[19] Been K, Jefferies MG. A state parameter for sands. Géotechnique 1985;35(2):99–112.
[20] Yang J, Sze HY. Cyclic strength of sand under sustained shear stress. J Geotech Geoenviron Eng 2011;137(12):1275–85.
[21] Shen CK, Vrymoed JL, Uyeno CK. The effects of fines on liquefaction of sands. In: Proceedings of the 9th international conference on soil mechanics and foundation engineering, Tokyo, Japan; 1977.
[22] Kuerbis RH, Negussey D, Vaid YP. Effect of gradation and fines content on the undrained response of sand. In: Proceedings of a specialty conference: hydraulic fill structures, Colorado State University, Fort Collins, Colorado, United States; 1988.
[23] Carraro JAH, Bandini P, Salgado R. Liquefaction resistance of clean and nonplastic silty sands based on cone penetration resistance. J Geotech Geoenviron Eng 2003;129(11):965–76.
[24] Xenaki VC, Athanasopoulos GA. Liquefaction resistance of sand–silt mixtures: an experimental investigation of the effect of fines. Soil Dyn Earthq Eng 2003;23(3):1–12.
[25] Dash HK, Sitharam TG. Undrained cyclic pore pressure response of sand–silt mixtures: effect of nonplastic fines and other parameters. Geotech Geol Eng 2009;27(4):501–17.
[26] Stamatopoulos CA. An experimental study of the liquefaction strength of silty sands in terms of the state parameter. Soil Dyn Earthq Eng 2010;30(8):662–78.
[27] Porcino D, Diano V. Laboratory study on pore pressure generation and liquefaction of low-plasticity silty sandy soils during the 2012 earthquake in Italy. J Geotech Geoenviron Eng. 2016;142(10):4016048.
[28] Wei X, Yang J. The effects of initial static shear stress on liquefaction resistance of silty sand. In: Proceedings of the 6th international conference on earthquake geotechnical engineering, Christchurch, New Zealand; 2015.
[29] Ladd R. Preparing test specimens using undercompaction. Geotech Test J 1978;1(1):16–23.
[30] Yang J, Savidis S, Roemer M. Evaluating liquefaction strength of partially saturated sand. J Geotech Geoenviron Eng 2004;130(9):975–9.
[31] Yang J, Wei LM. Collapse of loose sand with the addition of fines: the role of particle shape. Geotechnique 2012;62(12):1111–25.
[32] Sze H, Yang J. Failure modes of sand in undrained cyclic loading: impact of sample preparation. J Geotech Geoenviron Eng 2014;140(1):152–69.
[33] Yang J. Non-uniqueness of flow liquefaction line for loose sand. Géotechnique 2002;52(10):757–60.
[34] Yang J, Liu X. Shear wave velocity and stiffness of sand: the role of non-plastic fines. Géotechnique 2016;66(6):500–14.
[35] Sze HY. Initial shear and confining stress effects on cyclic behaviour and liquefaction resistance of sands [Ph.D. thesis]. The University of Hong Kong; 2010.
[36] Liang L-B. Static liquefaction of sand-fines mixtures with the presence of initial shear stress [MPhil thesis]. The University of Hong Kong; 2016.
[37] Yang J, Luo XD. Exploring the relationship between critical state and particle shape for granular materials. J Mech Phys Solids 2015;84:196–213.
[38] Yang J, Luo XD. The critical state friction angle of granular materials: does it depend on grading? Acta Geotech 2018;13(3):535–47.
[39] Wichtmann T, Niemunis A, Triantafyllidis T, Poblete M. Correlation of cyclic preloading with the liquefaction resistance. Soil Dyn Earthq Eng 2005;25(12):923–32.

[40] Finn WDL, Pickering DJ, Bransby PL. Sand liquefaction in triaxial and simple shear tests. J Soil Mech Found Div 1971;97(4):639–59.
[41] Seed HB, Peacock WH. Test procedures for measuring soil liquefaction characteristics. J Soil Mech Found Div 1971;97(8):1099–119.
[42] Rahman MM, Lo SR. The prediction of equivalent granular steady state line of loose sand with fines. Geomech Geoeng 2008;3(3):179–90.
[43] Yang J, Wei LM, Dai BB. State variables for silty sands: global void ratio or skeleton void ratio? Soils Found 2015;55(1):99–111.
[44] Luo XD, Yang J. Effects of fines on shear behavior of sand: a DEM analysis. In: Proceedings of the 5th international young geotechnical engineers' conference; 2, 265–8; 2013.